eLIFE elifesciences.org

RESEARCH ARTICLE

Figures and figure supplements

Dendritic mitochondria reach stable positions during circuit development

Michelle C Faits *et al*

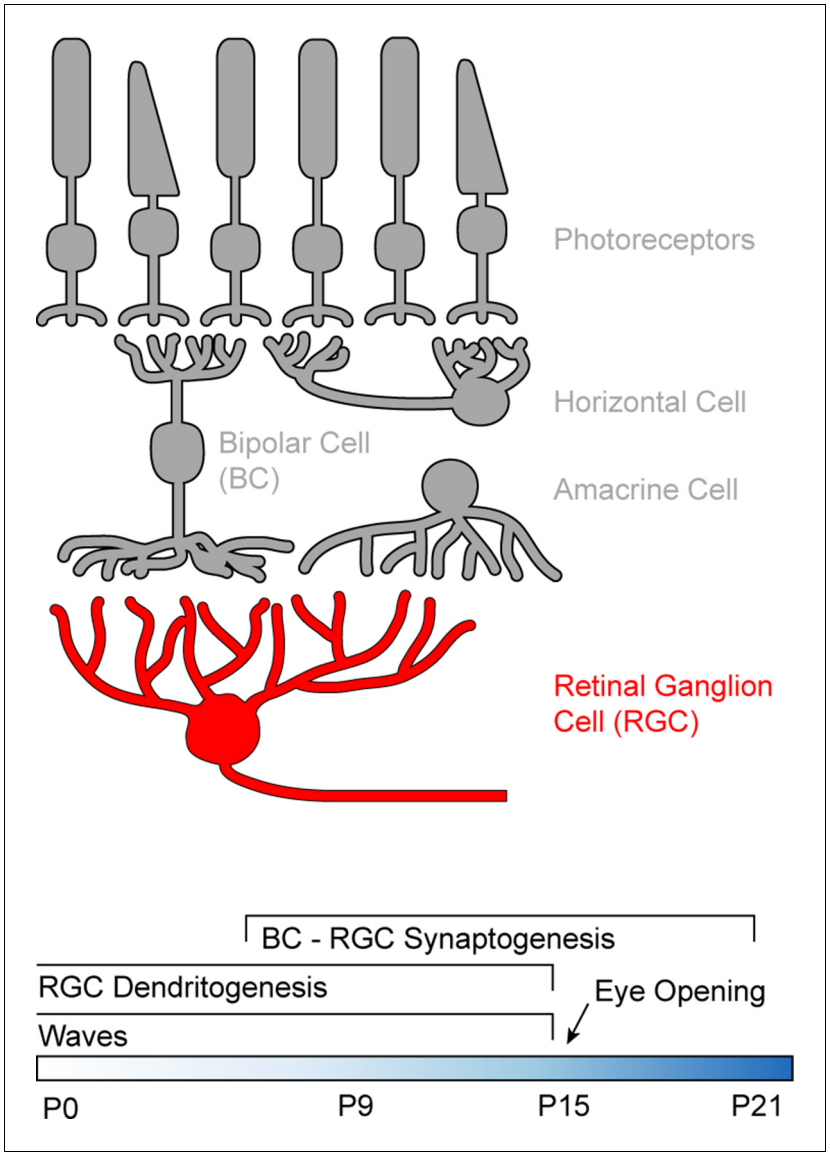

Figure 1. Schematic of the retinal circuitry and its development. *Top*: Illustration of the five classes of neurons in the mammalian retina. Photoreceptors - rods and cones indicated by the shape of their outer segments - translate changes in photon flux into changes in glutamate release. Horizontal cells provide feedback to photoreceptor terminals, whereas bipolar cells (BCs) relay photoreceptor signals from the outer to the inner retina where they provide excitatory input to a diverse class of inhibitory interneurons called amacrine cells and to retinal ganglion cells (RGCs), the output neurons of the eye. *Bottom*: Timeline of retinal development from birth (postnatal day 0) to circuit maturity (P21).

DOI: http://dx.doi.org/10.7554/eLife.11583.003

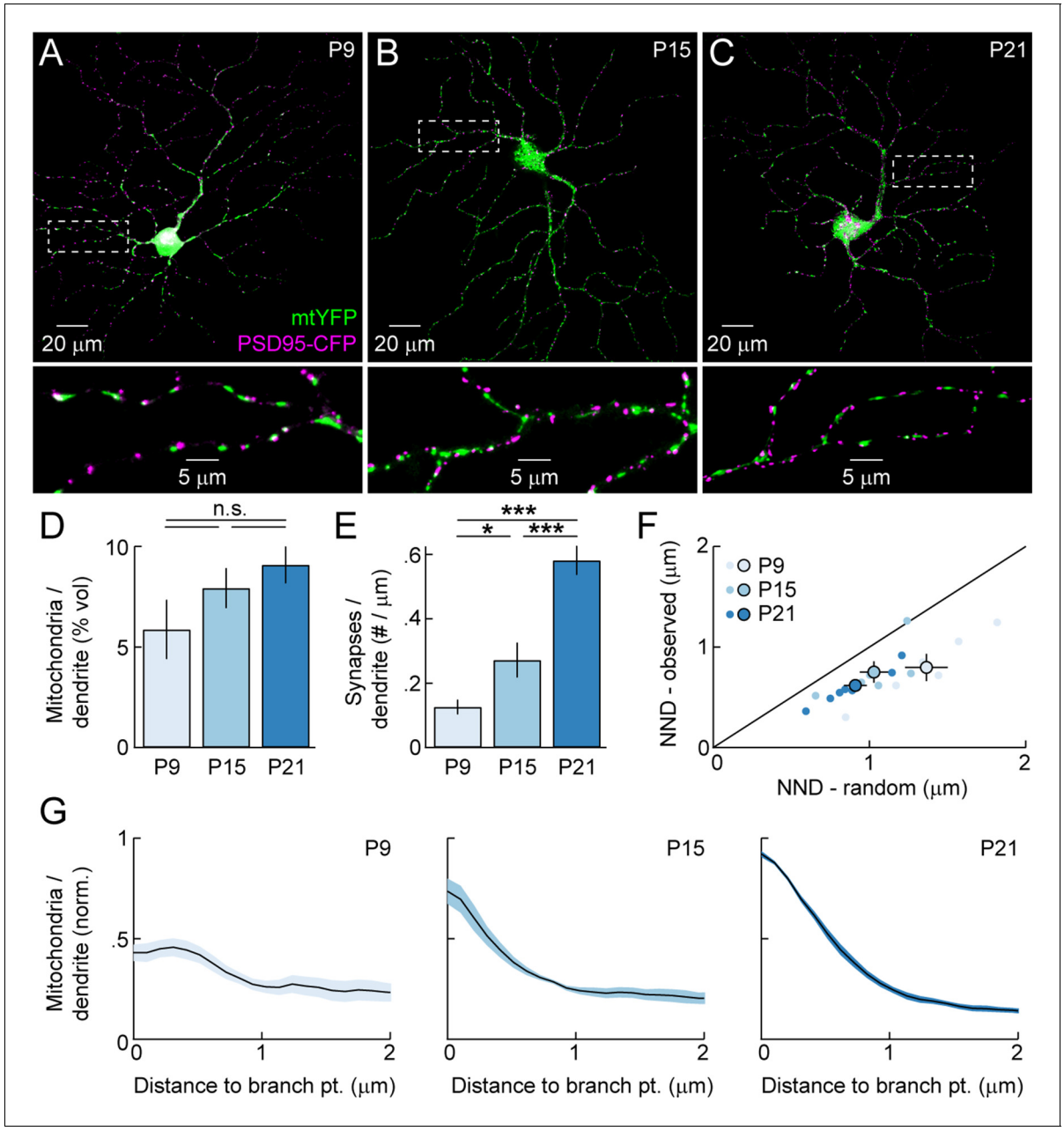

Figure 2. Mitochondrial distribution in RGC dendrites across development. (**A**–**C**) Representative RGCs expressing mtYFP and PSD95-CFP in P9 (**A**), P15 (**B**), and P21 (**C**) retinas. *Top panels* show maximum intensity projections (MIPs) through confocal image stacks and *bottom panels* show MIPs of excerpts of the same stacks at higher magnification. (**D**) Density of mitochondria in RGC dendrites expressed as a volumetric fraction (see 'Materials and methods') across development. (**E**) Density of synapses along RGC dendrites given per length of dendrite based on skeletonization of the respective arbors (see 'Materials and methods') across development. (**F**) Scatter plots comparing the average nearest neighbor distance from synapses to mitochondria (NND-observed) to the mean average NND obtained from Monte Carlo simulations in which the positions of synapses along dendrites were randomized (NND-random). *Dots* represent individual cells and *circles* (*error bars*) indicate the mean (± SEM) at the different ages examined. (**G**) Normalized mitochondrial density plotted as a function of distance from dendritic branch points at P9 (*left*), P15 (*middle*), and P21 (*right*). *Solid lines (shaded areas*) indicate the mean (± SEM) across a number of RGCs (P9 n = 6, P15, n = 6, P21, n = 8). mtYFP, mitochondrially targeted yellow fluorescent protein; RGC, retinal ganglion cell.

DOI: http://dx.doi.org/10.7554/eLife.11583.004

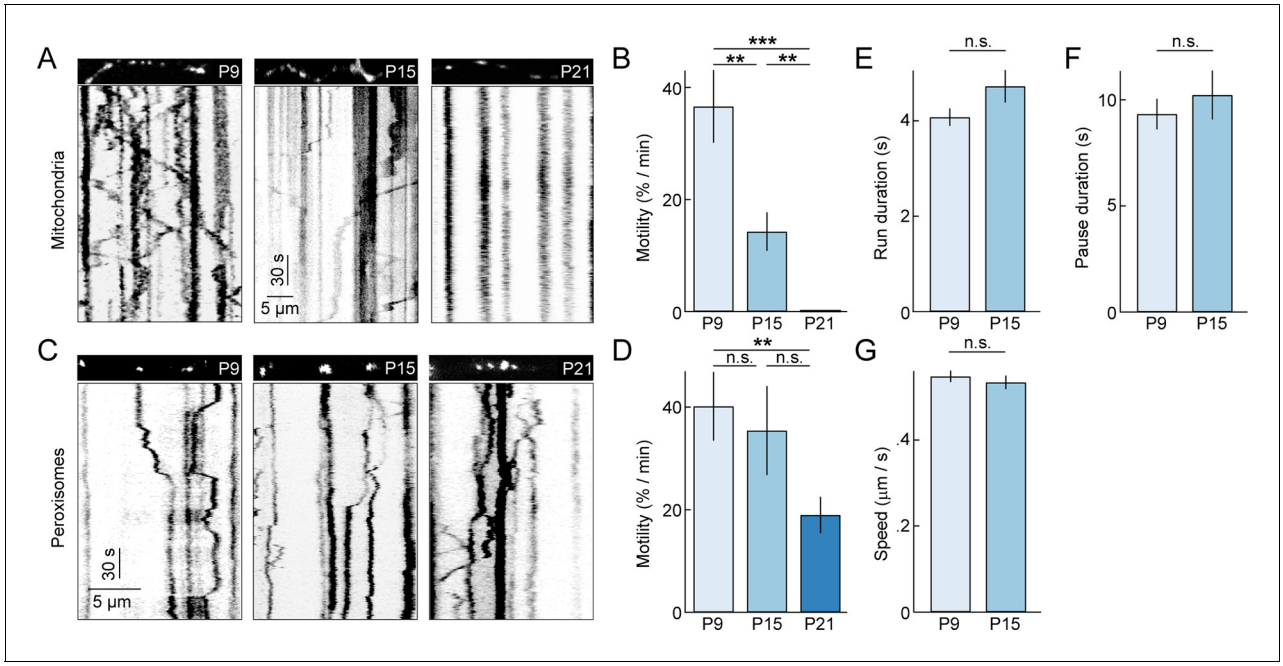

Figure 3. Motility of dendritic mitochondria and peroxisomes across development. (**A**) Kymographs of representative time-lapse imaging series of mitochondria (mtYFP, 0.9 fps, **A**) at P9 (*left*), P15 (*middle*), and P21 (*right*). *Top panels* show still frames at t = 0s of the branch segments depicted in the kymographs in the *bottom panels*. (**B**) Summary data of the motile fraction of mitochondria across development (P9 n = 10 RGCs, P15 n = 9 RGCs, P21 n = 7 RGCs). (**C**, **D**) Analogous to A (**C**) and B (**D**) but for time-lapse imaging of peroxisomes labeled with SKL-GFP (P9 n = 11 RGCs, P15 n = 10 RGCs, P21 n = 12 RGCs). (**E**–**G**) *Bars (error bars*) indicating the mean (± SEM) duration of uninterrupted runs (**E**), duration of pauses (**F**), and speed during uninterrupted motion (**G**) for mitochondria at P9 and P15 (P9 n = 65 mitochondria, P15 n = 32 mitochondria). See also ***Video 1***. mtYFP, mitochondrially targeted yellow fluorescent protein; RGCs, retinal ganglion cells.

DOI: http://dx.doi.org/10.7554/eLife.11583.006

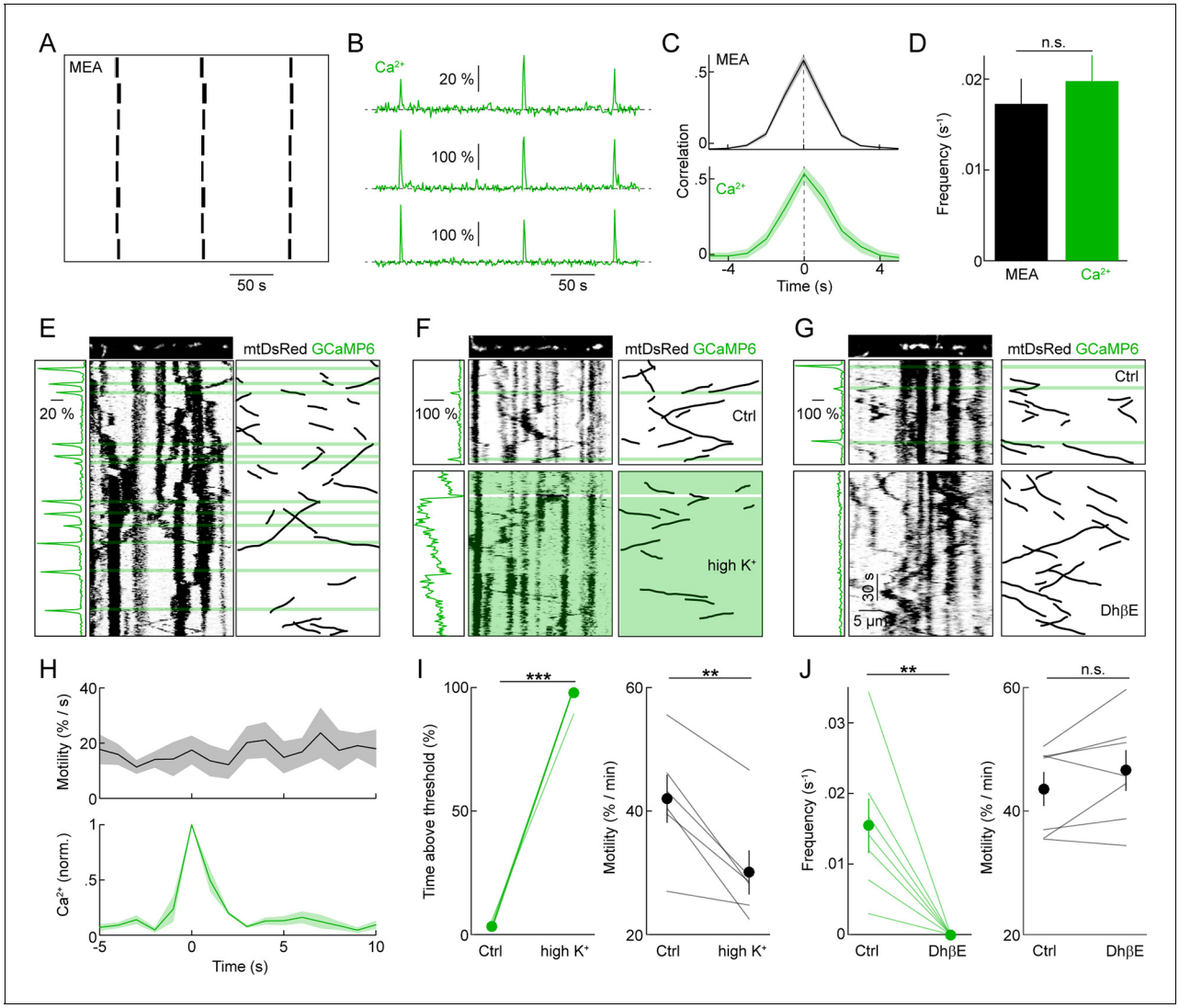

Figure 4. Spontaneous neuronal activity, dendritic Ca^{2+} transients, and mitochondrial motility during development. (**A**) Raster plot of representative spike trains of eight neighboring RGCs recorded in a biolistically labeled retinal explant on an MEA at P9. (**B**) Representative △F/F traces of GCaMP6s signals recorded from three neighboring RGCs by two-photon imaging. (**C**) Cross-correlations of firing rates (*top panel*) and dendritic Ca^{2+} transients (*bottom panel*) of neighboring RGCs (<200 µm between recording sites on MEA, <200 µm between cell bodies in Ca^{2+} imaging) (MEA recordings n = 30 pairs, Ca^{2+} imaging n = 11 pairs). (**D**) Average frequencies of waves of correlated activity on MEA (*black bar*) and global Ca^{2+} signals in RGC dendrites observed by two-photon imaging (*green bar*) in biolistically labeled retinal explants at P9 (MEA n = 6 retinas, Ca^{2+} imaging n = 22 retinas, p>0.6). (**E–G**) GCaMP6s and mtDsRed signals during simultaneous fast (0.9 fps) time-lapse two-photon imaging. *Top*: still frames of mtDsRed channel at t = 0s. *Left panels*: ΔF/F traces aligned with time plotted in kymograph. ΔF/F traces were calculated based on the average GCaMP6s intensity in the dendrite segment shown above the kymograph. *Center panels*: kymographs of mtDsRed signal. Green overlay indicates the timing Ca^{2+} transients. *Right panels*: black lines represent schematized depictions of mitochondrial runs in the kymographs. (**F**) Break between *top* and *bottom panels* represents 10 min between pre-treatment (*top*) and 30 mM K^+ application (*bottom*). (**G**) 5 µM DHβE treatment. (**H**) *Top*: Plot of the instantaneous mitochondrial motility as a function of time relative to a Ca^{2+} transient (n = 134 mitochondria, 10 RGCs). *Bottom*: Normalized Ca^{2+} imaging trace as a function of time (aligned on t = 0 as the time of the Ca^{2+} transient). *Lines (shaded areas)* represent the mean (± SEM). (**I, J**) Paired plots of RGCs before and after 30 mM K^+ (**I**) or DhβE (**J**) application. In the *left panel* of **I** the percentage of time above threshold measured was measured as percentage of frames in which the average GCaMP6s intensity within the frame was more than 2 SD above mean intensity of across the whole recording. The left panel of **J** show the frequency of Ca^{2+} transients. *Right panels* of **I** and **J** show changes in mitochondrial motility between pre-treatment and treatment portions of the recordings (30 mM K^+ n = 8 RGCs, DhβE n = 7 RGCs). RGCs, retinal ganglion cells.

DOI: http://dx.doi.org/10.7554/eLife.11583.008

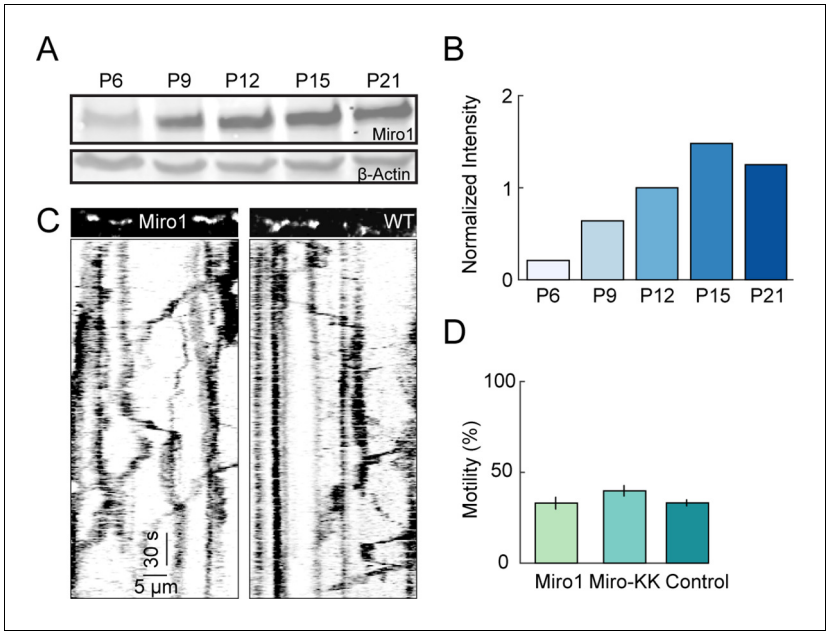

Figure 4—figure supplement 1. Miro1 expression and effect on mitochondrial motility in RGCs during development. (**A**) Western blot showing Miro1 protein expression levels in whole retinal lysate at P6 – P21. *Bottom panel* shows β-actin loading control. (**B**) *Bars* indicate the intensities of the western blot signal relative to β-actin intensity and normalized to P12 intensity level. (**C**) Kymographs of representative time-lapse imaging series of mitochondria (mtYFP, 0.9 fps) in P9 RGCs overexpressing Miro1 (*left*) or expressing mtYFP alone (*right*). *Top panels* show still frames at t = 0s of the branch segments depicted in the kymographs in the *bottom panels*. (**D**) Summary data of the motile fraction of mitochondria in RGCs overexpressing Miro1, a mutant form of Miro1 unable to bind Ca^{2+} (MiroKK), or mtYFP alone (control) (Miro1 n = 9 RGCs, MiroKK n = 4, control n = 6). fps, frames per second; mtYFP, mitochondrially targeted yellow fluorescent protein; RGC, retinal ganglion cell.
DOI: http://dx.doi.org/10.7554/eLife.11583.009

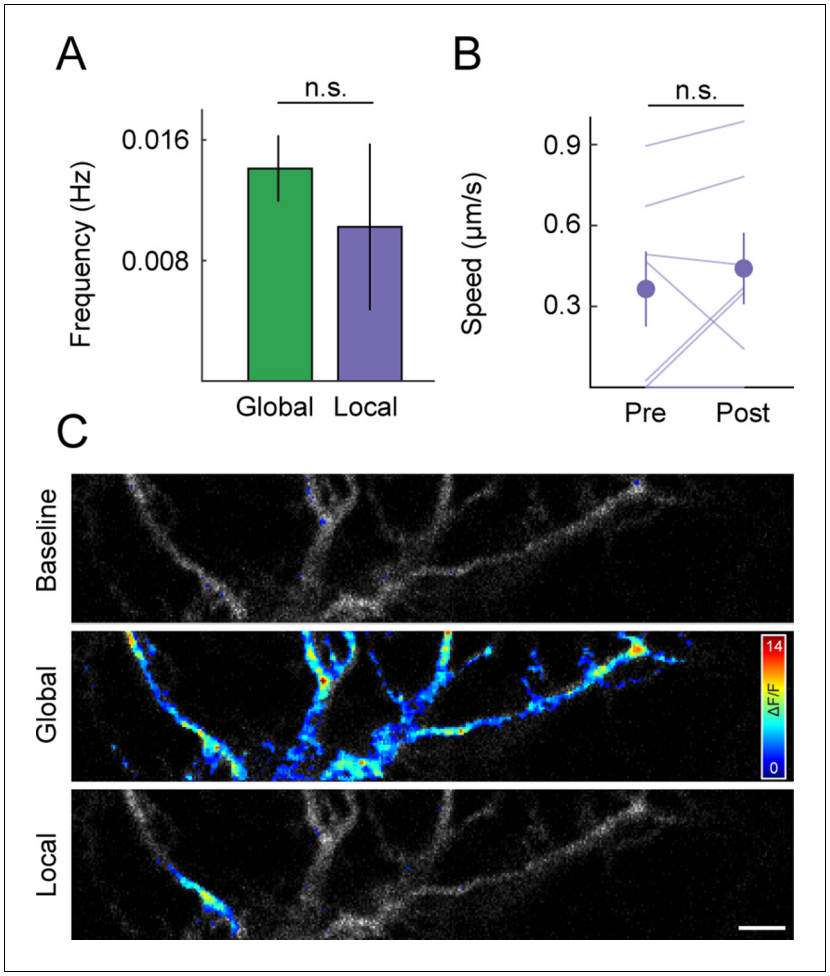

Figure 4—figure supplement 2. Spontaneous, local dendritic Ca^{2+} transients and mitochondrial motility during development. (**A**) *Bars (error bars)* indicating the mean (± SEM) frequency of global and local Ca^{2+} events in P9 RGCs (global n = 32 RGCs, local n = 7). (**B**) Paired plot of average mitochondrial speed in the 5 s before (Pre) and 5 s after (Post) a local Ca^{2+} event within a moving mitochondrion's path (n = 7 mitochondria). (**C**) Representative images of a P9 RGC dendritic branch during global and local signals. Heat maps of ΔF/F intensities are overlaid onto a maximum intensity projection of the GCaMP6 signal in all three panels. The *top panel* is a representative image of the baseline GCaMP6 intensity; the *middle panel* is a global Ca^{2+} event and the *bottom panel* shows a local Ca^{2+} transient. Scale bar: 5 µm. RGC, retinal ganglion cell.

DOI: http://dx.doi.org/10.7554/eLife.11583.010

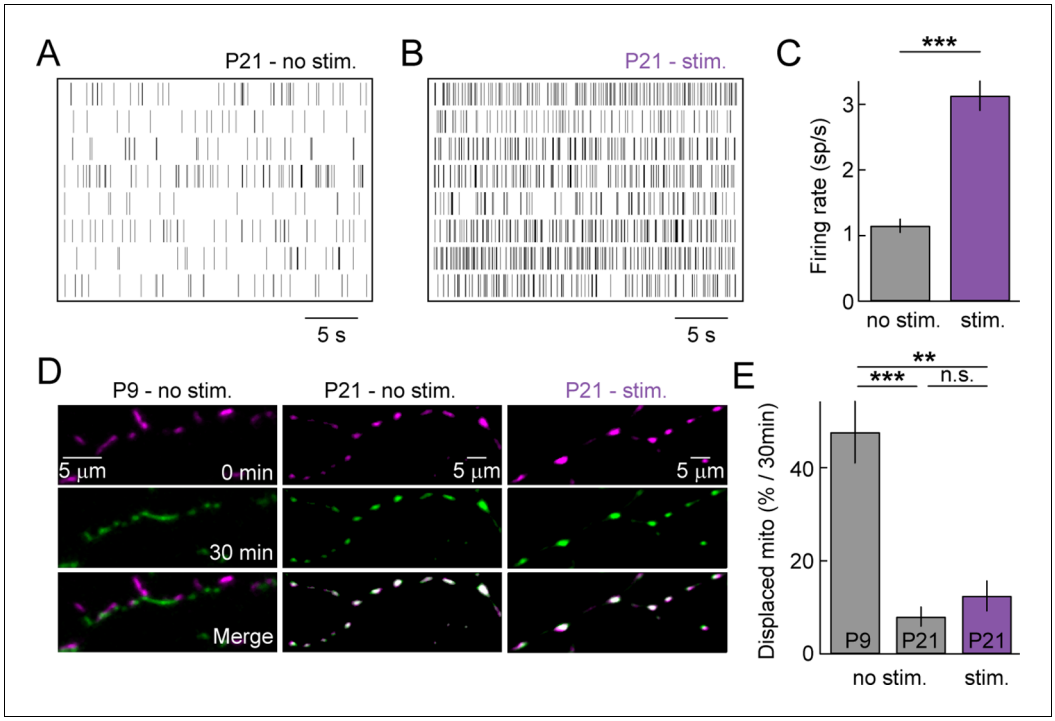

Figure 5. Sensory-evoked neuronal activity and mitochondrial motility at maturity. (**A**, **B**) Spike raster plots of eight representative RGCs recorded in darkness (**A**) and during presentation of a full-field white noise stimulus (**B**, see 'Materials and methods'). (**C**) *Bars (error bars*) indicate the mean (± SEM) firing rates of RGCs (n = 334 RGCs, 3 retinas, $p<10^{-26}$). (**D**) Representative RGCs expressing mtCFP at t = 0 min (*top panels*), t = 30 min (*middle panels*) after being exposed to white noise stimulus (*right panels*) or kept in darkness (*left and center panels). Bottom panels* show merged images of t = 0 and t = 30 min. (**E**) *Bars* (*error bars*) indicating the mean (± SEM) of % mitochondria displaced between t = 0 min and t = 30 min (P9 – no stim. n = 5 RGCs, P21 – no stim. n = 5 RGCs, P21 – stim n = 5 RGCs). RGCs, retinal ganglion cells.

DOI: http://dx.doi.org/10.7554/eLife.11583.013

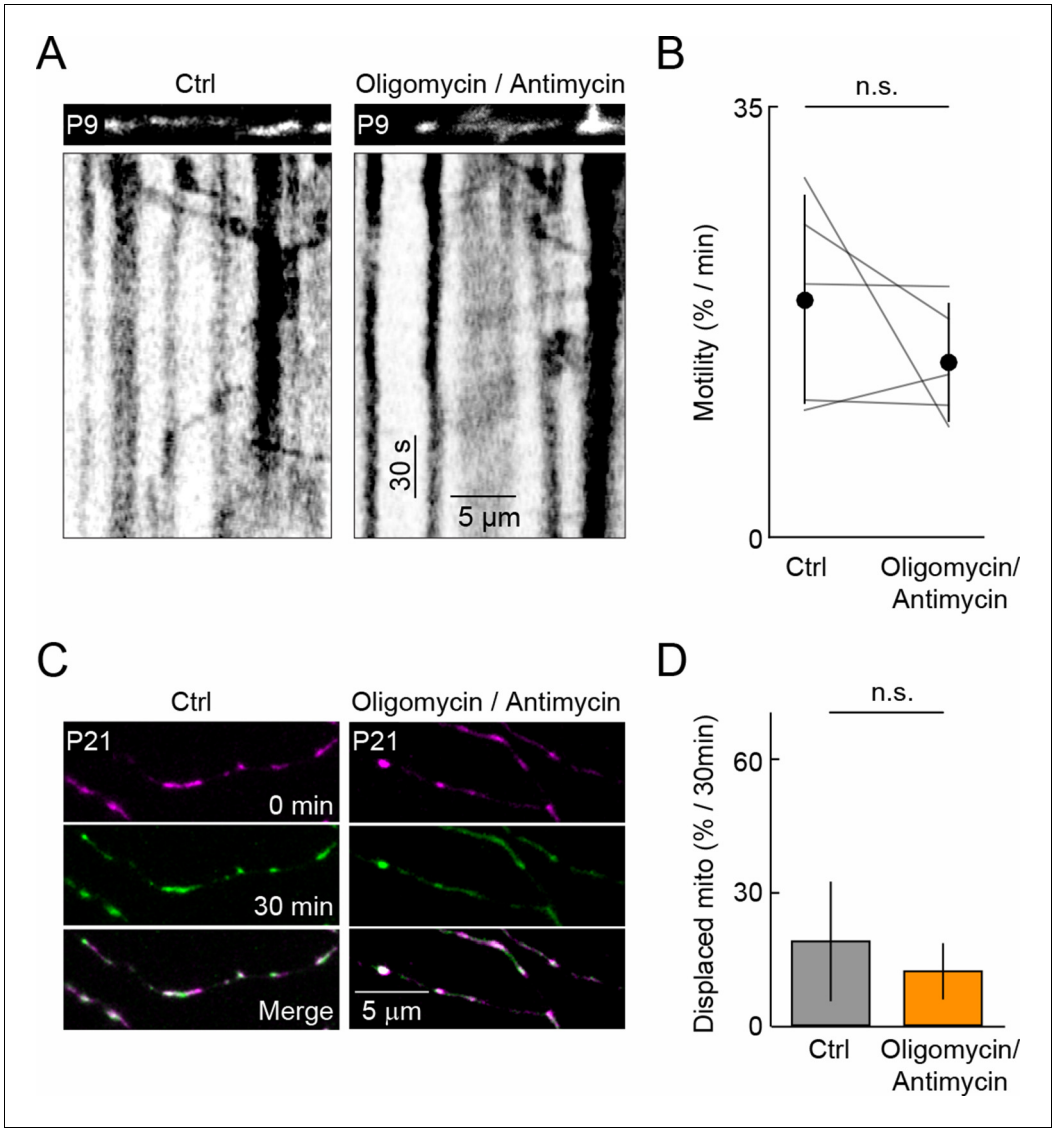

Figure 5—figure supplement 1. Antimycin A and Oligomycin and mitochondrial motility. (**A**) Kymographs of representative time-lapse imaging series of mitochondria (mtDsRed, 0.9 fps) in a P9 RGC before (*left*) and after Oligomycin/Antimycin A application. *Top panels* show still frames at t = 0s of the branch segments depicted in the kymographs in the *bottom panels*. (**B**) Paired plots of RGC mitochondrial motility before and after 30 min of 10 µM Oligomycin/ 4 µM Antimycin A application at P9 (n = 5 RGCs, p>0.2). (**C**) Representative images of P21 RGCs expressing mtDsRed at t = 0 min (*top panels*), t = 30 min (*middle panels*) in the presence (*right panels*) or absence (*left panels*) of Oligomycin/Antimycin A. *Bottom panels* show merged images of t = 0 and t = 30 min. (**D**) *Bars (error bars)* indicating the mean (± SEM) of % mitochondria displaced between t = 0 min and t = 30 min (n = 4 RGCs, p>0.4). fps, frames per second; RGC, retinal ganglion cell.

DOI: http://dx.doi.org/10.7554/eLife.11583.014

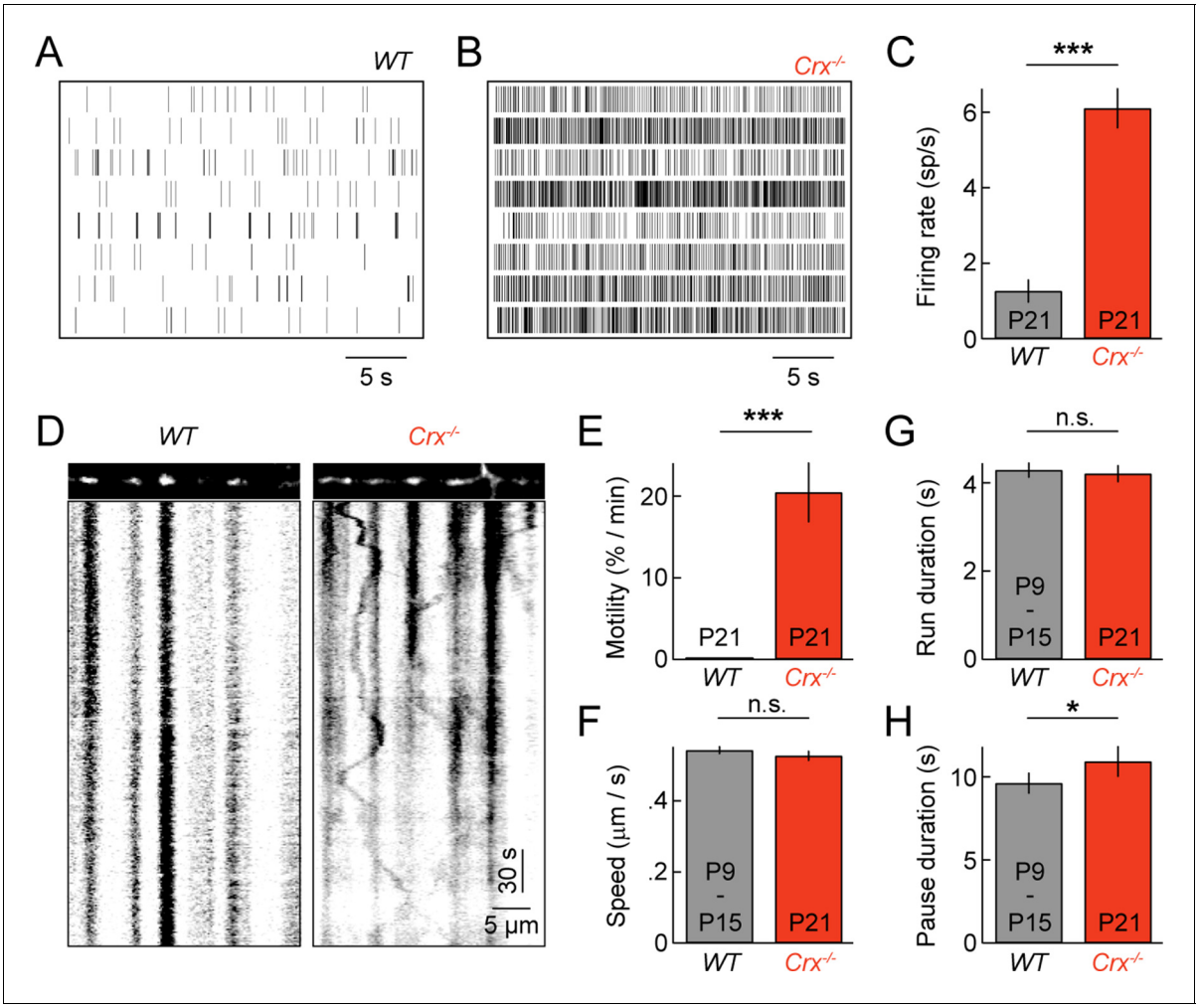

Figure 6. Pathological hyperactivity and dendritic mitochondria in retinal degeneration. (**A**, **B**) Spike raster plots of eight representative RGCs recorded from P21 *WT* (**A**) and from P21 *Crx*$^{-/-}$ retinas (**B**). (**C**) *Bars (error bars)* indicating the mean (± SEM) firing rates of *WT* and *Crx*$^{-/-}$ RGCs (*WT* n = 100 RGCs, 3 retinas, *Crx*$^{-/-}$ n = 235 RGCs, 3 retinas, $p<10^{-8}$). (**D**) Kymographs of representative time-lapse series of a P21 *WT* RGC (*left panels*) and *Crx*$^{-/-}$ RGC (*right panels*). (**E**) *Bars (error bars)* indicating the mean (± SEM) motile fraction of mitochondria in P21 WT and *Crx*$^{-/-}$ dendrites (P21 *WT* n = 7 RGCs, *Crx*$^{-/-}$ n = 6 RGCs). (**FH**) *Bars (error bars)* indicating the mean (± SEM) mitochondrial speed during uninterrupted motion (**F**), duration of uninterrupted runs (**G**), and duration of pauses (**H**) for mitochondria in P9 – 15 *WT* and *Crx*$^{-/-}$ dendrites (*Crx*$^{-/-}$ n = 30 mitochondria, pooled *WT* P9 and P15 n = 97 mitochondria). RGC, retinal ganglion cell.

DOI: http://dx.doi.org/10.7554/eLife.11583.015